bioRxiv preprint doi: https://doi.org/10.1101/2020.10.30.360925; this version posted October 30, 2020. The copyright holder for this preprint (which was not certified by peer review) is the author/funder, who has granted bioRxiv a license to display the preprint in perpetuity. It is made available under aCC-BY-NC-ND 4.0 International license.

Fine Molecular Tuning of Chimeric Antigen Receptors through Hinge Length Optimization

Scott McComb*[1-3], Tina Nguyen[1], Kevin A. Henry[1,3], Darin Bloemberg[1], Susanne Maclean[1], Rénald Gilbert[1,4], Christine Gadoury[1], Rob Pon[1], Traian Sulea[1,5], Qin Zhu[1], Risini D. Weeratna[1]

[1]Human Health Therapeutics Research Centre, National Research Council, Canada
[2]University of Ottawa Centre for Infection, Immunity and Inflammation, Department of Biochemistry, Microbiology, and Immunology, Faculty of Medicine, University of Ottawa, Ottawa, Canada
[3]Department of Biochemistry, Microbiology, and Immunology, Faculty of Medicine, University of Ottawa, Ottawa, Canada
[4]Department of Bioengineering, McGill University, Montréal, Québec, Canada
[5]Institute of Parasitology, McGill University, Sainte-Anne-de-Bellevue, QC H9X 3V9, Canada.

*Correspondence: scott.mccomb@nrc-cnrc.gc.ca

Running title: CAR Fine-tuning through Hinge Length Modulation

Keywords: CAR-T; cellular immunotherapy; molecular optimization; protein design; hinge element; CAR optimization

Declarations:

- The research presented in this manuscript is primary research conducted at and supported by the National Research Council of Canada. All listed authors have reviewed the data presented here, attest to the validity of the data, and approve its publication.
- All data and materials presented in the manuscript will be made available under reasonable terms
- Authors declare no competing interests

Contributions:

- SMc, TN, DB, KH, TS, RG and RW contributed to conceptualization, experimental design, analysis, and interpretation of results
- TN, DB, SMa, CG, RP, and QZ contributed to technical development, performed experiments, and compiled data.
- SMc, TN, KH, and RW contributed to writing and editing the manuscript

bioRxiv preprint doi: https://doi.org/10.1101/2020.10.30.360925; this version posted October 30, 2020. The copyright holder for this preprint (which was not certified by peer review) is the author/funder, who has granted bioRxiv a license to display the preprint in perpetuity. It is made available under aCC-BY-NC-ND 4.0 International license.

Abstract

Background: Chimeric antigen receptor (CAR) technology has revolutionized the treatment of B-cell malignancies and steady progress is being made towards CAR-immunotherapies for solid tumours. In the context of CARs targeting antigens which are commonly overexpressed in cancer but also expressed at lower levels in normal tissues, such as epidermal growth factor family receptors EGFR or HER2, it is imperative that any targeting strategy consider the potential for on-target off-tumour toxicity. Molecular optimization of the various protein domains of CARs can be used to increase the tumour selectivity.

Method: Herein, we utilize high-throughput CAR screening to identify a novel camelid single-domain antibody CAR (sdCAR) targeting human epidermal growth factor (EGFR) with high EGFR-specific activity. To further optimize the target selectivity of this EGFR-sdCAR, we performed progressive N-terminal single amino acid truncations of an extended human CD8 hinge domain [$(G4S)_3$GG-45CD8h] to improve selectivity for EGFR-overexpressing cells. We also make direct comparison of varying hinge domains in scFv-based CARs targeting EGFR-family tumour associated antigens EGFRvIII and HER2.

Results: Through comparison of various hinge-truncated scFv- and sdAb-based CARs, we show that the CAR hinge/spacer domain plays varying roles in modifying CAR signaling depending upon target epitope location. For membrane-proximal epitopes, hinge truncation by even a single amino acid resulted in fine control of CAR signaling strength. Hinge-modified CARs showed consistent and predictable signaling in Jurkat-CAR cells and primary human CAR-T cells in vitro and in vivo.

Conclusions: Overall, these results indicate that membrane-proximal epitope targeting CARs can be optimized through hinge length tuning for improved target selectivity and therapeutic function.

bioRxiv preprint doi: https://doi.org/10.1101/2020.10.30.360925; this version posted October 30, 2020. The copyright holder for this preprint (which was not certified by peer review) is the author/funder, who has granted bioRxiv a license to display the preprint in perpetuity. It is made available under aCC-BY-NC-ND 4.0 International license.

Background

Following the remarkable clinical success of CD19-targeted chimeric antigen receptor (CAR) therapies for the treatment of B-cell malignancies, design and development of novel CARs for more common solid tumours is a highly active area of research and development[1]. The first step for CAR-development is the identification of an antigen binding domain (ABD), typically composed of an antibody single-chain variable fragment[2,3], which can be used to create a CAR with low tonic activation and high target responsive activity. Previous work has also demonstrated that camelid single-domain antibodies (sdAb), also called V_HHs or nanobodies, can be used as effective CAR ABDs[4,5], and sdAb-CARs are now producing promising results in BCMA-sdAb targeted CAR-T therapy for myeloma[6,7]. Following identification of a functional ABD, molecular optimization can be used to further fine-tune the therapeutic properties of a CAR. All elements of the CAR molecule, including the ABD, hinge, transmembrane domain, and intracellular signaling domains, have been demonstrated to have significant impact on the signaling properties and functionality of CARs[2,3].

Recent work has shown for instance that decreased CAR signaling in CD19-specific CARs can be achieved by lowering the affinity of the ABD[8], altering the hinge or transmembrane domains[9–11], or engineering signaling domains with reduced activity[12]. Intriguingly, these diverse molecular strategies have consistently enhanced CAR-T persistence and therapeutic benefit in animal models and in at least one clinical trial thus far[8], suggesting that an optimal level of signaling may be somewhat lower than that of current generation clinical CD19-targeting CAR-T therapies. Thus, molecular optimization of CARs has emerged as a viable strategy for widening the therapeutic window of novel CAR-T therapies.

Epidermal growth factor receptor (EGFR) is one of the most commonly altered oncogenes in solid cancers, either through a variety of activating mutations or through over-expression of the native receptor[13,14]. EGFR has a relatively large extracellular domain with four subdomains[15], and is a

bioRxiv preprint doi: https://doi.org/10.1101/2020.10.30.360925; this version posted October 30, 2020. The copyright holder for this preprint (which was not certified by peer review) is the author/funder, who has granted bioRxiv a license to display the preprint in perpetuity. It is made available under aCC-BY-NC-ND 4.0 International license.

well-established target for monoclonal antibodies and small-molecule inhibitors[16,17]. EGFR has also been explored as a target for CAR-T therapy, and clinical trials have been undertaken using ABDs specific for either the WT[18,19] or a mutated tumour-specific form of the receptor known as EGFRvIII[20,21]. A flurry of recent clinical reports using EGFR-targeted CAR-T therapy in lung, biliary, and pancreatic cancers revealed no unmanageable toxicity and documented partial disease responses in some patients[22–25]. EGFR is also under investigation as a target for bi-specific immune engaging therapy[26].

As EGFR is expressed in normal tissues as well as on tumour cells it is imperative that any targeting strategy consider the potential for on-target off-tumour toxicity. In pre-clinical CAR-T work, it has previously been shown that the use of lower affinity EGFR or human epidermal growth factor 2 (HER2) ABDs for CAR-T can improve selectivity for overexpressing tumour cells over normal tissues[27]. Herein we present the development of a novel camelid single-domain antibody (sdAb) CAR targeting human EGFR, and demonstrate that fine optimization of the hinge domain can be used to carefully tune CAR signaling strength to enhance selectivity for antigen overexpressing tumours. Our results using EGFR-sdCAR and scFv-CARs targeting HER2 and EGFRvIII suggest that it may be possible to modify the hinges of CARs targeting membrane-proximal epitopes of other cancer associated antigens in order to optimize their signaling and tumour selectivity, minimize toxicity, and enhance CAR-T cell persistence.

Methods

CAR cloning

Three previously reported EGFR-specific sdAb sequences[28] were cloned into a modular CAR backbone using PCR amplification and single-pot restriction ligation as previously described[29]. EGFR-sdCAR constructs bearing either a full-length human 45 amino acid CD8 hinge (45CD8h) or progressively N-terminally truncated hinge variants (34CD8h, 22CD8h, or no hinge) were cloned using Gibson assembly.

bioRxiv preprint doi: https://doi.org/10.1101/2020.10.30.360925; this version posted October 30, 2020. The copyright holder for this preprint (which was not certified by peer review) is the author/funder, who has granted bioRxiv a license to display the preprint in perpetuity. It is made available under aCC-BY-NC-ND 4.0 International license.

A library of sdAb021-CAR truncation mutants with single amino acid N terminal truncations of the human CD8 hinge extended with an additional N-terminal flexible linker [$(GGGGS)_3$GG-CD8h] was generated using a modular hinge-CAR with convenient type-IIs restriction sites integrated into the construct 3' of the sdAb coding region. An array of DNA encoding truncated CD8 hinge domains of varying lengths (60 to 1 amino acid) was synthesized as DNA fragments (Twist Bioscience, USA) and cloned into the sdAb021-modular-hinge-BBz-GFP CAR construct using single-pot restriction ligation. Limited hinge truncation libraries with defined-target CARs were generated by exchanging the sdAb021 sequence with appropriate scFv sequences. Trastuzumab derived scFv sequences were generated based on previously reported mutant forms of trastuzumab with enhanced avidity[40], whereas EGFRvIII-targeting scFvs were generated as previously reported[29]. Both HER2- and EGFRvIII-scFvs were in a VH-$(G4S)_3$-VL format.

Cell lines and culture

All cell lines were purchased from American Tissue Culture Collection (ATCC, Manassas, VA). The glioblastoma cell line U97MG-WT and U87MG-vIII (U87-vIII, expressing EGFRvIII via retroviral transduction and sorting) were kindly provided by Professor Cavnee, from the Ludwig Institute for Cancer Research, University of California, San Diego (San Diego, CA, USA)[45]. Cell lines used were Jurkat, and target cells SKOV-3, MCF-7, U-87-MG vIII, Raji, and Nalm6. Target cells were transduced with lentivirus containing NucLight Red (Sartorius, Essen BioScience, USA), a third generation HIV-based, VSV-G pseudotyped lentivirus encoding a nuclear-localized mKate2. All cell lines were cultured in RPMI supplemented with 10% fetal calf serum and 1% penicillin/streptomycin. These cell lines were tested for the presence of mycoplasma contamination by PCR.

CAR-J assay

bioRxiv preprint doi: https://doi.org/10.1101/2020.10.30.360925; this version posted October 30, 2020. The copyright holder for this preprint (which was not certified by peer review) is the author/funder, who has granted bioRxiv a license to display the preprint in perpetuity. It is made available under aCC-BY-NC-ND 4.0 International license.

Jurkat cells were transfected via electroporation according to a previously outlined protocol[29] . Briefly, 5x10^5 cells were suspended in 100 ul Buffer 1SM (5 mM KCl, 15 mM $MgCl_2$, 120 mM Na_2HPO_4/NaH_2PO_4, 25 mM sodium succinate, and 25 mM mannitol; pH7.2) and incubated with 2µg of pSLCAR-CAR plasmids as described in the text or with no plasmid control. Cells and plasmid DNA in solution were transferred into 0.2 cm generic electroporation cuvettes (Biorad Gene Pulser; Bio-Rad Laboratories, Hercules, California, USA) and immediately electroporated using a Lonza Nucleofector I (Lonza, Basel, Switzerland) and program X-05 (X-005 on newer Nucleofector models). Cells were cultured in pre-warmed recovery media (RPMI containing 20% FBS, 1mM sodium pyruvate and 2 mM L-glutamine) for four 4h before being co-cultured with EGFR-expressing target cells U-87MG-vIII, MCF7 and SC-OV-3 or negative control Ramos and Nalm6. Electroporated Jurkat cells were added to varying numbers of target cells in round bottom 96-well plates in effector to target (E:T) ratios ranging from 1:10 to 100:1 (effector to target ratio) or with no target cells (or an E:T of 1:0) and cultured overnight before being staining with allophycocyanin (APC)-conjugated anti human-CD69 antibody (BD Biosciences #555533). Flow cytometry was performed using a BD- Fortessa (BD Biosciences) and data was analyzed using Flowjo software (Flowjo LLC, Ashland, Oregon, USA) and visualized using GraphPad Prism (GraphPad Software, Inc. California, USA).

Human peripheral blood mononuclear cell (PBMC) isolation

Heparinized whole blood was collected from healthy donors by venipuncture and transported at room temperature from Ottawa Hospital Research Institute. Blood was diluted 1:1 with Hank's balanced salt solution (HBSS) and PBMCs were isolated by Ficoll density gradient centrifugation. Briefly, samples layered on Ficoll gradient were centrifuged for 20 min at 700 x g without applying a brake. The PBMC interface was carefully removed by pipetting and was washed twice with HBSS by stepwise centrifugation for 15 min at 300 x g. PBMC were resuspended and counted by mixed 1:1 with Cellometer

bioRxiv preprint doi: https://doi.org/10.1101/2020.10.30.360925; this version posted October 30, 2020. The copyright holder for this preprint (which was not certified by peer review) is the author/funder, who has granted bioRxiv a license to display the preprint in perpetuity. It is made available under aCC-BY-NC-ND 4.0 International license.

ViaStain™ acridine orange/propidium iodide (AOPI) staining solution and counted using a Nexcelom Cellometer Auto 2000 (Nexcelom BioScience, Lawrence, Massachusetts, USA).

T cells from freshly isolated PBMCs were activated with Miltenyi MACS GMP TransAct CD3/CD28 beads and seeded at 1×10^6 cells/ml in serum-free StemCell Immunocult-XF media (StemCell Technologies, Vancouver, Canada) containing clinical grade human IL-2 (20 U/ml, Novartis) or Miltenyi TexMACS containing research grade human IL-7 and human IL-15 (both 10 ng/ml).

T cells from freshly isolated PBMC were activated with Miltenyi MACS GMP TransAct CD3/CD28 beads and seeded 1x10^6 T cells/ml in serum-free StemCell Immunocult-XF media (StemCell Technologies, Vancouver, Canada) with clinical grade 20U/ml human IL-2 (Novartis) or Miltenyi TexMACS with research grade 10 ng/ml human IL-7 and 10 ng/ml human IL-15.

Human primary T transduction by spinfection

High concentration lentiviral particles encoding various sdCAR constructs were generated as previously described [29]. After 24 h of T cell stimulation with beads, T cells were transduced with sdCAR-GFP lentiviral vectors (multiplicity of infection = 10) by spinfection. Briefly, lentivirus was added to T cells (1×10^6 cells/ml) and the mixture was centrifuged at 850 × g for 2 h at 32°C. After centrifugation, cells were incubated at 37°C for another 2 h. After incubation, cells were plated in a 24 well plate (100,000 cells/ml/well in a total of 1.5mL) in media supplemented with cytokine(s). Media with cytokine(s) was added at 48 and 72 h post transduction to promote CAR-T cell proliferation without disrupting the cells. CAR-T cells were sampled daily until the end of production. Cell number and viability were assessed by AOPI staining and counting using a Nexcelom Cellometer. CAR-T cells were propagated until harvest on days 7, 9, 14, and 21 to assess the efficiency of transduction and to characterize T cell subpopulations by flow cytometry. CAR-T cells that had returned to a resting state (as determined by decreased growth

bioRxiv preprint doi: https://doi.org/10.1101/2020.10.30.360925; this version posted October 30, 2020. The copyright holder for this preprint (which was not certified by peer review) is the author/funder, who has granted bioRxiv a license to display the preprint in perpetuity. It is made available under aCC-BY-NC-ND 4.0 International license.

kinetics, day 10 post-T cell activation) were used for assays. Expression of GFP-CARs by transduced T cells ranged from 20% to 70%.

Continuous live-cell imaging cytotoxicity assay

Cytotoxicity of the CAR-T cells was assayed using a Sartorius IncuCyte S3 (Essen Bioscience). Tumour cells (U87vIII-NucLight, MCF7-NucLight, and SKOV3-NucLight were plated in a flat bottom 96-well plate (2000 cells/well). CAR-T cells or control T cells were added into each well in a final volume of 200 µl per well at varying effector:target ratios and co-cultured for 7 days at 37°C. Images were taken every 30 min in light phase and under red (ex. 565-605 nm; em. 625-705 nm) or green fluorescence (ex. 440-480 nm; em. 504-544 nm). The assays were repeated twice with T cells derived from independent blood donors.. For one donor, CAR-T cells challenged once or twice with EGFR-high SKOV3 cells were rechallenged with various freshly plated target cells after 7 day of co-culture. Automated cell counting of red (target) or green (CAR-T) cells was performed using Incucyte analysis software and data were graphed using GraphPad Prism.

Animal studies

NOD/SCID/IL2Ry$^{-/-}$ (NSG, JAX #005557) mice were purchased from Jackson Laboratories and maintained by the Animal Resource Group at the National Research Council of Canada.. Eight-week-old NSG mice were injected with 2x10^6 SKOV-3 in 100 ul of PBS subcutaneously. Eighteen days post tumourtumour cells injection (when tumourtumour reached 5mm x 5mm), mice were retro orbitally injected with 5x10^6 mock T cells or T cells transduced with various CAR-T cells as described in the text. TumourTumours were measured using calipers twice a week and mice were imaged via IVS in vivo imager for red-fluorescence signal (expressed on tumour cells) once a week. For the alternative U87vIII model experiments, mice were subcutaneously injected with 1x10^6 fluorescently labelled U87-vIII cells described above, a number we previously determined to consistently produce a palpable tumour within

bioRxiv preprint doi: https://doi.org/10.1101/2020.10.30.360925; this version posted October 30, 2020. The copyright holder for this preprint (which was not certified by peer review) is the author/funder, who has granted bioRxiv a license to display the preprint in perpetuity. It is made available under aCC-BY-NC-ND 4.0 International license.

7 days. Eight days after tumour cell injection, cryo-preserved CAR-T cells were thawed, washed with PBS, and $1x10^7$ total T cells (with 20-25% CAR transduction) were immediately delivered intra-tumourally, ensuring equal distribution of tumour sizes between groups. Tumour growth was evaluated three times per week using calipers by trained animal technicians blinded to specific treatment groups. Primary endpoint was tumour size above $2000mm^3$, with secondary endpoints determined by overall animal health and well-being. Mice were also assessed for tumour growth using IVIS in vivo imaging to examine red fluorescence derived from the NLS-mKate2 marked U87vIII cells. Mice were euthanized when they met pre-specified endpoints. The study was approved by the NRC-HHT Institutional Animal Care Committee and was conducted in accordance with Canadian Councol on Animal Care (CCAC) guidelines. Tumour growth and survival (humane endpoint) curves were generated using GraphPad Prism.

Flow cytometry and antibodies

Blood was obtained from mice at various time points post CAR-T injection. Blood was washed with cold PBS and pelleted at 350 × g for 5 min at 4°C. Red blood cells were lysed using Red Blood Cell Lysing Buffer Hybri-Max (Sigma-Aldrich, St. Louis, MO, USA). Human T cells were identified and analyzed for activation/differentiation status using the following antibodies: hCD45-APC-H7, hCD45RA-BV650, hCD45RO-PE-CF594, hCD27-BUV737, hCCR7-PE, hCD4-BUV395, and hCD8-PerCP-Cy5.5 (all antibodies from BD Biosciences, USA). CAR expression was measured indirectly via expression of GFP incorporated in CAR constructs. To evaluate exhaustion, staining by an hPD-1-BV421 antibody was evaluated. T cell activation was detected using hCD25-PE-Cy7 and hCD69-BV786 antibodies. For in vivo studies, a BV711-labeled antibody against mouse CD45 was used to identify murine cells and CD19 expression was analyzed using an anti-human CD19-BUV496 antibody. Staining of human EGFR was performed using anti-human EGFR-PE-CF594 (BD Biosciences, Cat #563431).

Results

bioRxiv preprint doi: https://doi.org/10.1101/2020.10.30.360925; this version posted October 30, 2020. The copyright holder for this preprint (which was not certified by peer review) is the author/funder, who has granted bioRxiv a license to display the preprint in perpetuity. It is made available under aCC-BY-NC-ND 4.0 International license.

High-affinity EGFR-specific sdAbs generate antigen-responsive CARs with low tonic signaling

Camelid sdAbs were raised in a previous study against EGFR using DNA immunization and phage display[28]. In order to assess whether these sdAbs were functional in the context of a sdCAR (see Supplementary Fig. 6 for an overview of the workflow employed here) we chose three EGFR-specific sdAbs with varying affinities and epitopes (Table 1)[28]. The sdAbs were cloned into a modular CAR backbone and the resulting sdCARs were screened for responses to target cells with varying EGFR expression using a previously described high throughput Jurkat screening assay[29] (Fig. 1A). Jurkat cells electroporated with any of three EGFR-specific sdCAR constructs showed specific upregulation of CD69 following co-culture with EGFR-high SKOV3 cells or EGFR-low MCF7 cells (Fig. 1B,C and Supplementary Fig. 1). In contrast, Jurkat cells expressing EGFR sdCARs showed no activation in response to EGFR-negative Raji cells (Fig. 1D). These data confirmed that high affinity EGFR sdAbs can effectively redirect CAR signaling towards EGFR-expressing cell lines.

Hinge shortening decreases CAR signaling

It has previously been shown that altering the length of the spacer (hinge) between the ABD and transmembrane domain can be used to modulate CAR signaling[30,31]. Thus, we next investigated whether the selectivity of the EGFR sdCARs for EGFR-high cells could be increased by progressively decreasing the length of the hinge region. We cloned EGFR sdCAR constructs with either a full-length 45 amino acid human CD8 hinge (45CD8h) or progressively N-terminally truncated hinge variants (34CD8h, 22CD8h, or no hinge) (Fig. 2A). Jurkat cells transiently expressing the truncated hinge variants of all three EGFR sdCARs showed progressively decreasing activation in response to EGFR-high SKOV3 cells (Fig. 2B-D). Intriguingly, EGFR sdCAR responses to EGFR-low MCF7 cells appeared to be more sensitive to hinge truncation, particularly for the sdAb021 sdCAR (Fig. 2B-D, Supplementary Fig. 2).

bioRxiv preprint doi: https://doi.org/10.1101/2020.10.30.360925; this version posted October 30, 2020. The copyright holder for this preprint (which was not certified by peer review) is the author/funder, who has granted bioRxiv a license to display the preprint in perpetuity. It is made available under aCC-BY-NC-ND 4.0 International license.

We wanted to more finely map the effects of hinge length modulation on an EGFR sdAb CAR. As a starting point we designed an extended hinge domain wherein an additional N-terminal flexible linker of 17 amino acids was included before the human CD8-hinge sequence [$(GGGGS)_3$GG-CD8h]. We then generated a library of sdAb021-CAR constructs with single amino acid N-terminal deletions of the human CD8 hinge. Screening our sdCAR single-residue hinge truncation library revealed a clear pattern of CAR activation (Fig 3A). CAR constructs containing a hinge domain of a full human CD8-hinge or longer produced a consistently high response to SKOV3 cells. Interestingly, addition of a short SGG N-terminal linker slightly increased CAR signaling against EGFR-high SKOV3 and EGFR-low MCF7 cells. CARs with CD8 hinge sizes between 39 and 32 amino acids showed a progressive decrease in CAR activation, while CAR constructs with hinges less than 26 residues showed no apparent difference in CAR-specific response between EGFR-high target and EGFR-negative controls. As in experiments above, it appeared that CAR activation fell more quickly in MCF7 cells relative to SKOV3, providing a range of CAR constructs wherein response to SKOV3 remains but MCF7-response is not significantly different from response to irrelevant target cells (NALM6). We also re-examined our data, isolating tonic (target-independent) signaling and response to EGFR-negative NALM6 cells; we observed no consistent trend in antigen independent activation of constructs with varying hinge length (Supplementary Fig. 3). Taken together, these data suggest that fine hinge mapping may be an effective strategy to optimize CAR selectivity for EGFR-overexpressing tumours.

Epitope location is critical determinant of CAR hinge sensitivity

As has been previously proposed, the location of the CAR target epitope should be critical in determining the minimal hinge length necessary for CAR signaling[32]. We do not have definitive data as to the epitope(s) targeted by the EGFR sdAbs used in our sdCAR constructs, though epitope binning experiments indicated that all three sdAbs have partially overlapping epitopes, and cross-reactivity analysis is suggestive of membrane proximal domain IV binding[28] (Table 1). To more carefully

bioRxiv preprint doi: https://doi.org/10.1101/2020.10.30.360925; this version posted October 30, 2020. The copyright holder for this preprint (which was not certified by peer review) is the author/funder, who has granted bioRxiv a license to display the preprint in perpetuity. It is made available under aCC-BY-NC-ND 4.0 International license.

investigate the role of epitope location, we generated limited hinge libraries for CARs with known target epitopes. We generated scFv-CARs based on either trastuzumab, which is known to bind a highly membrane proximal epitope of HER2 [33], or novel EGFRvIII-specific antibodies[29], which by necessity must bind the membrane distal neo-epitope of EGFRvIII (Table 1). As hypothesized, the trastuzumab CAR required a very long hinge element: no HER2 scFv CARs containing shorter than a full CD8-hinge showed any response (Fig. 3B). In contrast, membrane-distal targeting EGFRvIII CARs maintained full activation when the entire CD8 hinge domain was deleted (Fig. 3C). These data clearly demonstrated that epitope location is a key determinant of the hinge length required for maximal CAR signaling.

Hinge-truncated CAR signaling is consistent in primary T cells in vitro and in vivo

We next wished to confirm whether the reduced signaling of sdCARs with truncated hinge elements expressed in Jurkat cells was also manifested in primary CAR-T cells. Thus, we transduced T cells derived from two human blood donors with hinge-modified forms of the sdAb021 sdCAR. Following polyclonal expansion and sdCAR transduction, green fluorescent protein (GFP)+ CAR-T cells with various hinge elements were placed in low density co-culture with target cells stably marked with a nuclear localized red fluorescent protein. Co-cultures were then monitored for tumour cell (red fluorescence) and CAR-T cell (green fluorescence) expansion over 7 days. Consistent with observations in Jurkat cells, hinge truncation progressively diminished the ability of sdAb021 sdCARs to restrict tumour cell growth (Fig. 4A,B) and expand in response to target cells (Fig. 4C,D). Also consistent with Jurkat observations, there was no obvious relationship between hinge length and CAR tonic signaling as measured by CAR-T expansion with no additional stimulation (Supplementary Fig. 4A,B). Most importantly, although all hinge truncated sdAb-021 sdCARs were able to control expansion of EGFR-high SKOV3 cells, only the sdCAR with the unmodified hinge (sdAb021-45CD8h-28z) showed potent tumour killing and CAR-T expansion in response to EGFR-low MCF7 cells (Fig. 4B,D).

bioRxiv preprint doi: https://doi.org/10.1101/2020.10.30.360925; this version posted October 30, 2020. The copyright holder for this preprint (which was not certified by peer review) is the author/funder, who has granted bioRxiv a license to display the preprint in perpetuity. It is made available under aCC-BY-NC-ND 4.0 International license.

We next wished to more finely examine the effect of hinge truncation under a wider variety of antigenic conditions. Thus, we plated hinge-modified sdAb021 sdCAR-T cells with EGFR-very high (SKOV3), EGFR-medium/high (U87vIII), or EGFR-low (MCF7) target cells at varying effector:target ratios and examined them using live microscopy. Using primary T cells from both donors, sdCAR-T cells with truncated hinges maintained tumour killing and CAR-T expansion in response to EGFR-overexpressing SKOV3 and U87vIII cells but showed low responses to EGFR-low MCF7 cells (Fig. 4E). Overall, these data indicate that hinge length modulation, and specifically progressive hinge truncation, can be used to decrease responses of primary CAR-T cells against cells with varying target expression and increase selectivity for antigen overexpressing cells.

Hinge-truncated CARs maintain selectivity for high-expressing cells following re-challenge

We next investigated the effect of hinge truncation on serial CAR-T killing. We isolated hinge modified sdCAR-T cells following primary challenge with antigen-overexpressing SKOV3 cells using the low density co-culture assay as described above and re-challenged the sdCAR-T cells by re-plating with additional target cells (Fig. 5A-C). Re-challenged cells maintained their relative ability to kill target cells, which also decreased with hinge length (Fig. 5B). Re-plating secondary challenge cells for a tertiary challenge revealed a similar trend in maintained tumour repression decreasing this hinge length (Fig. 5C). While target killing was mostly maintained following re-challenge, we observed a consistent decrease in CAR-T expansion in secondary and tertiary re-challenge assays (Fig. 5D-F).

To specifically address the question of whether sdCARs with truncated hinges maintained their selectivity following antigen experience, single or double SKOV3-challenged sdCAR-T cells were re-challenged with U87vIII (Fig. 5G-J) or MCF7 cells (Fig. 5K-N). Similar to SKOV3 serial challenge, re-challenged sdCAR-T cells of all hinge lengths showed decreased tumour killing and CAR-T expansion in response to both cell lines with reduced EGFR expression. These results indicated that re-stimulated

bioRxiv preprint doi: https://doi.org/10.1101/2020.10.30.360925; this version posted October 30, 2020. The copyright holder for this preprint (which was not certified by peer review) is the author/funder, who has granted bioRxiv a license to display the preprint in perpetuity. It is made available under aCC-BY-NC-ND 4.0 International license.

CAR-T cells show similar or higher antigenic discrimination as observed in primary challenge, with progressively decreasing antigen-induced expansion following serial challenge.

In vivo CAR-T response is progressively diminished with hinge truncation

Finally, we wished to investigate whether our in vitro observations regarding the relationship between hinge length and CAR-T activity were consistent in an in vivo xenograft model. Using the relatively slow growing SKOV3 model, mice were challenged with 2 million tumour cells subcutaneously and then treated intravenously at day 18 post-tumour implantation with 5 million hinge modified sdCAR-T cells or 1.25-1.5 million mock transduced CAR-T cells. There was a progressive increase in tumour growth in all mice (Fig. 6A) and decreased survival was observed in mice treated with hinge-truncated sdCAR-T cells (Fig. 6B). Surprisingly, mice treated with sdCAR-T cells bearing the shortest hinge (sdAb021-22CD8h-28z) showed apparent decreased survival compared with untreated animals, although larger experiments would be needed to confirm this result. The progressive effect of hinge truncation could be clearly observed in the final tumour volume measurement taken at day 112 post tumour challenge (Fig. 6C,D) prior to early experimental termination due to non-experiment related facility disruptions.

Examining CAR-T cells in the blood of treated mice revealed a consistent pattern of increased expansion of sdCAR-T cells with longer hinge regions at 43 and 54 days post-tumour injection (Fig. 6E). Analysis of T cell differentiation revealed increased naïve sdCAR-T cell and decreased effector sdCAR-T cell populations were for hinge truncated sdCARs (Fig. 6F), supporting the interpretation that truncated sdCAR-T cells show progressively decreased in in vivo responses. We also performed a similar experiment in which wild-type or hinge modified sdCAR-T cells were delivered intratumourally in the relatively more aggressive U87vIII glioblastoma xenograft model. We observed similar progressive decreases in anti-tumoural effect (Supplementary Fig. 5A-C) and CAR-T expansion (Supplementary Fig. 5D) and progressive increases in naïve CAR-T cell populations associated with hinge truncation

bioRxiv preprint doi: https://doi.org/10.1101/2020.10.30.360925; this version posted October 30, 2020. The copyright holder for this preprint (which was not certified by peer review) is the author/funder, who has granted bioRxiv a license to display the preprint in perpetuity. It is made available under aCC-BY-NC-ND 4.0 International license.

(Supplementary Fig. 5D). Taken together, these results demonstrated that hinge truncation can be used to reduce CAR-T signaling activity in vivo.

Discussion

We sought here to develop a novel CAR construct able to effectively target cells overexpressing EGFR and to discriminate between high level expression on tumours and lower expression on normal cells. Despite some variation in binding affinity for the three EGFR sdAb moieties tested here (Table 1), all three sdCAR constructs showed strong responses to EGFR-high SKOV3 and EGFR-low MCF7 target cells. Intriguingly, all EGFR-sdAb CAR receptors showed responsiveness to MCF7 cells despite no apparent reactivity of the purified sdAbs to EGFR-low MCF7 cells[28]. These results are consistent with previous observations that EGFR specific CARs are relatively insensitive to ABD affinity up to the micromolar range[27] and underscore the exquisite antigen sensitivity of CAR-T cells to respond to and lyse even very low antigen expressing target cells[34–36]. This phenomenon possibly relates to the extreme multi-valency of both CAR and EGFR on their respective cells. Increased valency is well known to lead to significant avidity effects that boost the apparent affinity of biological interactions[37–40], and these would presumably apply to CAR-T cells as well.

While CAR constructs with maximal antigen sensitivity might be desirable in certain contexts, such as for CAR-T therapies targeting B cell family restricted antigens, the presence of EGFR expression on normal tissue requires a targeting strategy that would be selective for EGFR-overexpressing cancer cells. Previously, affinity modulation has been used to increase selectivity of CAR constructs for overexpressing cells[27]. While it is certainly possible to decrease sdAb affinity through various molecular strategies[41], mutational antibody changes can sometimes lead to unpredictable binding behaviour such as unexpected off-target binding, elevated tonic signaling, or loss of efficacy. Thus, we wished to pursue an alternate strategy to decrease on target activity through hinge modification. The

bioRxiv preprint doi: https://doi.org/10.1101/2020.10.30.360925; this version posted October 30, 2020. The copyright holder for this preprint (which was not certified by peer review) is the author/funder, who has granted bioRxiv a license to display the preprint in perpetuity. It is made available under aCC-BY-NC-ND 4.0 International license.

use of hinge domains derived from various antibody isotypes or receptor ectodomains has been well-documented to have powerful influence on the ultimate signaling produced by a particular CAR construct[2], and the strategy of hinge truncation has also been previously explored[3,30,42,43].

Here, we extended the results of these previous studies to show that even very small truncations of a human CD8 hinge, down to the level of individual amino acids, can be a powerful and remarkably precise tuning mechanism for CAR signaling. For the EGFR sdCAR we tested most carefully, there was a sharp drop-off of CAR signaling over a range of only 10 amino acids within the CD8 hinge motif. While the requirements of lentiviral production and primary T cell transduction dictated that we could only test a limited number of constructs in primary T cells, it would be intriguing to map the optimal hinge length for antigen induced CAR-T killing or CAR-T expansion in genuine donor-derived T cells. Our hinge-truncation data using either membrane proximal (trastuzumab) or membrane-distal (anti-EGFRvIII-mAbs) based CAR constructs provides a clear demonstration of the criticality of epitope location as a determinant of hinge-sensitivity for CAR molecules reacting to tumour cells.

While the exact epitope for the EGFR sdAbs tested is not known, the data here would indicate a likely membrane proximal location. Consistent with this, sdAb028 cross-reacts with human and mouse but not cynomolgus EGFR; the only positions at which mouse and human EGFR sequences are identical but diverge from cynomolgus EGFR are in domain IV of EGFR[28]. Our finding that a full length CD8 hinge is required for the trastuzumab scFv-CAR seems to be consistent with previous experiments using similar CARs where hinge domains were also included[44], although it is worth noting that the scFv employed there diverges somewhat from that used here. In contrast to hinge truncation, we found that alonger than necessary hinge does not have a very deleterious effect on CAR signaling, at least as determined by the CAR-J assay. Previous work has indicated that longer hinges can decrease in vivo activity for membrane-distal epitope targeting CARs[42], but follow-up studies pinpointed the effect to be related to FC-binding by IgG-hinge motifs rather than hinge length specifically[43]. For those membrane-

bioRxiv preprint doi: https://doi.org/10.1101/2020.10.30.360925; this version posted October 30, 2020. The copyright holder for this preprint (which was not certified by peer review) is the author/funder, who has granted bioRxiv a license to display the preprint in perpetuity. It is made available under aCC-BY-NC-ND 4.0 International license.

proximal targeting CARs where a hinge is required though, our data demonstrates that CD8-hinge truncation is a powerful molecular strategy to reduce CAR-antigen sensitivity without the need to alter the ABD.

Due to the relatively more demanding technical requirements of testing CAR-T constructs in primary T cells we only tested a limited number of CAR constructs. Nonetheless, data presented here provide additional evidence that molecular optimization using transient CAR expression in Jurkat cells is predictive of signaling in stably transduced primary CAR-T cells, as we have previously reported[29]. The wider use of such optimization methodology could lead to improved ABD/hinge design for future CAR products. It may be possible for instance to design CARs with customized signaling for application in CD4, CD8, gamma-delta T cells, or NK cells.

The in vivo experiments presented here underline the fundamental trade-off between on-target, on-tumour activity and strategies that might reduce on-target off-tumour signaling. Achieving a level of signaling that is adequate for potent tumour killing yet also eliminates the risk of on-target toxicity may be difficult. Although in isolation, the SKOV3-selective truncated EGFR-sdAb CARs which were tested here had relatively little therapeutic effect in vivo it may be possible to combine such reduced signal hinge-truncated EGFR-sdCAR in a multi-antigen targeting CAR strategy that will ultimately more effectively recognize and lyse tumour cells in a highly selective fashion. Importantly, the aggressive xenograft models used here are imperfect and would likely not perfectly predict CAR-T signaling and activity in humans with slower growing and/or metastatic disease. The clinical use of CARs with varying hinge lengths could also present an intriguing alternative safety pathway for clinical trials of solid tumour targeting CARs through hinge length escalation.

bioRxiv preprint doi: https://doi.org/10.1101/2020.10.30.360925; this version posted October 30, 2020. The copyright holder for this preprint (which was not certified by peer review) is the author/funder, who has granted bioRxiv a license to display the preprint in perpetuity. It is made available under aCC-BY-NC-ND 4.0 International license.

Reference List

1. June CH, O'Connor RS, Kawalekar OU, Ghassemi S, Milone MC. CAR T cell immunotherapy for human cancer. Science. 2018;359:1361–5.

2. Srivastava S, Riddell SR. Engineering CAR-T Cells: Design Concepts. Trends Immunol. 2015;36:494–502.

3. Guedan S, Calderon H, Posey AD, Maus MV. Engineering and Design of Chimeric Antigen Receptors. Mol Ther Methods Clin Dev. 2018;12:145–56.

4. Wong WY, Tanha J, Krishnan L, Tian B, Kumar P, Gaspar K, et al. Abstract A74: CAR-T cells harboring camelid single domain antibody as targeting agent to CEACAM6 antigen in pancreatic cancer. Cancer Immunol Res. American Association for Cancer Research; 2017;5:A74–A74.

5. Yang EY, Shah K. Nanobodies: Next Generation of Cancer Diagnostics and Therapeutics. Front Oncol [Internet]. Frontiers; 2020 [cited 2020 Oct 2];10. Available from: https://www.frontiersin.org/articles/10.3389/fonc.2020.01182/full

6. Zhao W-H, Liu J, Wang B-Y, Chen Y-X, Cao X-M, Yang Y, et al. A phase 1, open-label study of LCAR-B38M, a chimeric antigen receptor T cell therapy directed against B cell maturation antigen, in patients with relapsed or refractory multiple myeloma. J Hematol OncolJ Hematol Oncol. 2018;11:141.

7. Madduri D. Results from CARTITUDE-1: A Phase 1b/2 Study of JNJ-4528, a CAR-T Cell Therapy Directed Against B-Cell Maturation Antigen (BCMA), in Patients with Relapsed and/or Refractory Multiple Myeloma (R/R MM). ASH; 2019 [cited 2020 Jan 7]. Available from: https://ash.confex.com/ash/2019/webprogram/Paper121731.html

8. Ghorashian S, Kramer AM, Onuoha S, Wright G, Bartram J, Richardson R, et al. Enhanced CAR T cell expansion and prolonged persistence in pediatric patients with ALL treated with a low-affinity CD19 CAR. Nat Med. 2019;25:1408–14.

9. Alabanza L, Pegues M, Geldres C, Shi V, Wiltzius JJW, Sievers SA, et al. Function of Novel Anti-CD19 Chimeric Antigen Receptors with Human Variable Regions Is Affected by Hinge and Transmembrane Domains. Mol Ther. 2017;25:2452–65.

10. Schäfer D, Henze J, Pfeifer R, Schleicher A, Brauner J, Mockel-Tenbrinck N, et al. A Novel Siglec-4 Derived Spacer Improves the Functionality of CAR T Cells Against Membrane-Proximal Epitopes. Front Immunol. 2020;11:1704.

11. Guest RD, Hawkins RE, Kirillova N, Cheadle EJ, Arnold J, O'Neill A, et al. The role of extracellular spacer regions in the optimal design of chimeric immune receptors: evaluation of four different scFvs and antigens. J Immunother Hagerstown Md 1997. 2005;28:203–11.

12. Feucht J, Sun J, Eyquem J, Ho Y-J, Zhao Z, Leibold J, et al. Calibration of CAR activation potential directs alternative T cell fates and therapeutic potency. Nat Med. 2019;25:82–8.

13. Thomas R, Weihua Z. Rethink of EGFR in Cancer With Its Kinase Independent Function on Board. Front Oncol [Internet]. Frontiers; 2019 [cited 2020 Jul 21];9. Available from: https://www.frontiersin.org/articles/10.3389/fonc.2019.00800/full#B1

bioRxiv preprint doi: https://doi.org/10.1101/2020.10.30.360925; this version posted October 30, 2020. The copyright holder for this preprint (which was not certified by peer review) is the author/funder, who has granted bioRxiv a license to display the preprint in perpetuity. It is made available under aCC-BY-NC-ND 4.0 International license.

14. Santarius T, Shipley J, Brewer D, Stratton MR, Cooper CS. A census of amplified and overexpressed human cancer genes. Nat Rev Cancer. Nature Publishing Group; 2010;10:59–64.

15. Ferguson KM. A structure-based view of Epidermal Growth Factor Receptor regulation. Annu Rev Biophys. 2008;37:353–73.

16. García-Foncillas J, Sunakawa Y, Aderka D, Wainberg Z, Ronga P, Witzler P, et al. Distinguishing Features of Cetuximab and Panitumumab in Colorectal Cancer and Other Solid Tumors. Front Oncol [Internet]. Frontiers; 2019 [cited 2020 Jul 21];9. Available from: https://www.frontiersin.org/articles/10.3389/fonc.2019.00849/full

17. Maennling AE, Tur MK, Niebert M, Klockenbring T, Zeppernick F, Gattenlöhner S, et al. Molecular Targeting Therapy against EGFR Family in Breast Cancer: Progress and Future Potentials. Cancers. Multidisciplinary Digital Publishing Institute; 2019;11:1826.

18. Martinez M, Moon EK. CAR T Cells for Solid Tumors: New Strategies for Finding, Infiltrating, and Surviving in the Tumor Microenvironment. Front Immunol [Internet]. 2019 [cited 2019 Sep 26];10. Available from: https://www.frontiersin.org/articles/10.3389/fimmu.2019.00128/full

19. Li J, Li W, Huang K, Zhang Y, Kupfer G, Zhao Q. Chimeric antigen receptor T cell (CAR-T) immunotherapy for solid tumors: lessons learned and strategies for moving forward. J Hematol OncolJ Hematol Oncol [Internet]. 2018 [cited 2020 Aug 25];11. Available from: https://www.ncbi.nlm.nih.gov/pmc/articles/PMC5809840/

20. Morgan RA, Johnson LA, Davis JL, Zheng Z, Woolard KD, Reap EA, et al. Recognition of Glioma Stem Cells by Genetically Modified T Cells Targeting EGFRvIII and Development of Adoptive Cell Therapy for Glioma. Hum Gene Ther. 2012;23:1043–53.

21. O'Rourke DM, Nasrallah MP, Desai A, Melenhorst JJ, Mansfield K, Morrissette JJD, et al. A single dose of peripherally infused EGFRvIII-directed CAR T cells mediates antigen loss and induces adaptive resistance in patients with recurrent glioblastoma. Sci Transl Med. 2017;9:eaaa0984.

22. Feng K, Guo Y, Liu Y, Dai H, Wang Y, Lv H, et al. Cocktail treatment with EGFR-specific and CD133-specific chimeric antigen receptor-modified T cells in a patient with advanced cholangiocarcinoma. J Hematol OncolJ Hematol Oncol [Internet]. 2017 [cited 2020 Aug 25];10. Available from: https://www.ncbi.nlm.nih.gov/pmc/articles/PMC5217546/

23. Feng K, Guo Y, Dai H, Wang Y, Li X, Jia H, et al. Chimeric antigen receptor-modified T cells for the immunotherapy of patients with EGFR-expressing advanced relapsed/refractory non-small cell lung cancer. Sci China Life Sci. 2016;59:468–79.

24. Liu Y, Guo Y, Wu Z, Feng K, Tong C, Wang Y, et al. Anti-EGFR chimeric antigen receptor-modified T cells in metastatic pancreatic carcinoma: A phase I clinical trial. Cytotherapy [Internet]. 2020 [cited 2020 Aug 25]; Available from: http://www.sciencedirect.com/science/article/pii/S1465324920306174

25. Guo Y, Feng K, Liu Y, Wu Z, Dai H, Yang Q, et al. Phase I Study of Chimeric Antigen Receptor–Modified T Cells in Patients with EGFR-Positive Advanced Biliary Tract Cancers. Clin Cancer Res. 2018;24:1277–86.

bioRxiv preprint doi: https://doi.org/10.1101/2020.10.30.360925; this version posted October 30, 2020. The copyright holder for this preprint (which was not certified by peer review) is the author/funder, who has granted bioRxiv a license to display the preprint in perpetuity. It is made available under aCC-BY-NC-ND 4.0 International license.

26. Suurs FV, Lub-de Hooge MN, de Vries EGE, de Groot DJA. A review of bispecific antibodies and antibody constructs in oncology and clinical challenges. Pharmacol Ther. 2019;201:103–19.

27. Liu X, Jiang S, Fang C, Yang S, Olalere D, Pequignot EC, et al. Affinity-tuned ErbB2 or EGFR chimeric antigen receptor T cells exhibit an increased therapeutic index against tumors in mice. Cancer Res. 2015;75:3596–607.

28. Rossotti MA, Henry KA, van Faassen H, Tanha J, Callaghan D, Hussack G, et al. Camelid single-domain antibodies raised by DNA immunization are potent inhibitors of EGFR signaling. Biochem J. Portland Press; 2019;476:39–50.

29. Bloemberg D, Nguyen T, MacLean S, Zafer A, Gadoury C, Gurnani K, et al. A High-Throughput Method for Characterizing Novel Chimeric Antigen Receptors in Jurkat Cells. Mol Ther - Methods Clin Dev [Internet]. 2020 [cited 2020 Jan 31]; Available from: http://www.sciencedirect.com/science/article/pii/S2329050120300231

30. Watanabe N, Bajgain P, Sukumaran S, Ansari S, Heslop HE, Rooney CM, et al. Fine-tuning the CAR spacer improves T-cell potency. OncoImmunology. 2016;5:e1253656.

31. Moritz D, Groner B. A spacer region between the single chain antibody- and the CD3 zeta-chain domain of chimeric T cell receptor components is required for efficient ligand binding and signaling activity. Gene Ther. 1995;2:539–46.

32. Qin L, Lai Y, Zhao R, Wei X, Weng J, Lai P, et al. Incorporation of a hinge domain improves the expansion of chimeric antigen receptor T cells. J Hematol OncolJ Hematol Oncol. 2017;10:68.

33. Garrett JT, Rawale S, Allen SD, Phillips G, Forni G, Morris JC, et al. Novel Engineered Trastuzumab Conformational Epitopes Demonstrate In Vitro and In Vivo Antitumor Properties against HER-2/neu. J Immunol. American Association of Immunologists; 2007;178:7120–31.

34. Stone JD, Aggen DH, Schietinger A, Schreiber H, Kranz DM. A sensitivity scale for targeting T cells with chimeric antigen receptors (CARs) and bispecific T-cell Engagers (BiTEs). Oncoimmunology. 2012;1:863–73.

35. Bluhm J, Kieback E, Marino SF, Oden F, Westermann J, Chmielewski M, et al. CAR T Cells with Enhanced Sensitivity to B Cell Maturation Antigen for the Targeting of B Cell Non-Hodgkin's Lymphoma and Multiple Myeloma. Mol Ther. Elsevier; 2018;26:1906–20.

36. Nerreter T, Letschert S, Götz R, Doose S, Danhof S, Einsele H, et al. Super-resolution microscopy reveals ultra-low CD19 expression on myeloma cells that triggers elimination by CD19 CAR-T. Nat Commun. Nature Publishing Group; 2019;10:1–11.

37. Vauquelin G, Charlton SJ. Exploring avidity: understanding the potential gains in functional affinity and target residence time of bivalent and heterobivalent ligands. Br J Pharmacol. 2013;168:1771–85.

38. Rudnick SI, Lou J, Shaller CC, Tang Y, Klein-Szanto AJP, Weiner LM, et al. Influence of Affinity and Antigen Internalization on the Uptake and Penetration of Anti-HER2 Antibodies in Solid Tumors. Cancer Res. 2011;71:2250–9.

bioRxiv preprint doi: https://doi.org/10.1101/2020.10.30.360925; this version posted October 30, 2020. The copyright holder for this preprint (which was not certified by peer review) is the author/funder, who has granted bioRxiv a license to display the preprint in perpetuity. It is made available under aCC-BY-NC-ND 4.0 International license.

39. Zhang J, Tanha J, Hirama T, Khieu NH, To R, Tong-Sevinc H, et al. Pentamerization of single-domain antibodies from phage libraries: a novel strategy for the rapid generation of high-avidity antibody reagents. J Mol Biol. 2004;335:49–56.

40. Zwaagstra JC, Sulea T, Baardsnes J, Radinovic S, Cepero-Donates Y, Robert A, et al. Binding and functional profiling of antibody mutants guides selection of optimal candidates as antibody drug conjugates. PLoS ONE [Internet]. 2019 [cited 2020 Aug 28];14. Available from: https://www.ncbi.nlm.nih.gov/pmc/articles/PMC6938348/

41. Alonso-Camino V, Sánchez-Martín D, Compte M, Nuñez-Prado N, Diaz RM, Vile R, et al. CARbodies: Human Antibodies Against Cell Surface Tumor Antigens Selected From Repertoires Displayed on T Cell Chimeric Antigen Receptors. Mol Ther - Nucleic Acids [Internet]. 2013 [cited 2018 Aug 30];2. Available from: https://www.cell.com/molecular-therapy-family/nucleic-acids/abstract/S2162-2531(16)30151-2

42. Hudecek M, Lupo-Stanghellini M-T, Kosasih PL, Sommermeyer D, Jensen MC, Rader C, et al. Receptor affinity and extracellular domain modifications affect tumor recognition by ROR1-specific chimeric antigen receptor T-cells. Clin Cancer Res Off J Am Assoc Cancer Res. 2013;19:3153–64.

43. Hudecek M, Sommermeyer D, Kosasih PL, Silva-Benedict A, Liu L, Rader C, et al. The non-signaling extracellular spacer domain of chimeric antigen receptors is decisive for in vivo antitumor activity. Cancer Immunol Res. 2015;3:125–35.

44. Zhao Y, Wang QJ, Yang S, Kochenderfer JN, Zheng Z, Zhong X, et al. A Herceptin-Based Chimeric Antigen Receptor with Modified Signaling Domains Leads to Enhanced Survival of Transduced T Lymphocytes and Antitumor Activity. J Immunol Baltim Md 1950. 2009;183:5563–74.

45. Abulrob A, Giuseppin S, Andrade MF, McDermid A, Moreno M, Stanimirovic D. Interactions of EGFR and caveolin-1 in human glioblastoma cells: evidence that tyrosine phosphorylation regulates EGFR association with caveolae. Oncogene. Nature Publishing Group; 2004;23:6967–79.

46. Pohlmann PR, Mayer IA, Mernaugh R. Resistance to Trastuzumab in Breast Cancer. Clin Cancer Res Off J Am Assoc Cancer Res. 2009;15:7479–91.

bioRxiv preprint doi: https://doi.org/10.1101/2020.10.30.360925; this version posted October 30, 2020. The copyright holder for this preprint (which was not certified by peer review) is the author/funder, who has granted bioRxiv a license to display the preprint in perpetuity. It is made available under aCC-BY-NC-ND 4.0 International license.

Table 1. Antigen-binding domains tested as CAR elements in this study.

Antibody Name	Type	Target	Affinity (K_D)	Cross-Reactivity	Epitope	Epitope Location	Ref
sdAb021	sdAb	EGFR (Erbb1)	38.5 nM	Human, Cyno	A; partial overlap with B	Unknown	[28]
sdAb027	sdAb	EGFR (Erbb1)	1.6 nM	Human, Cyno	A; partial overlap with B	Unknown	[28]
sdAb028	sdAb	EGFR (Erbb1)	9.0 nM	Human, Mouse	B; partial overlap with A	Unknown	[28]
Trastuzumab	scFv	HER2 (Erbb2)	n.d. (5 nM)[a]	Human, Cyno	Juxtamembrane conformational epitope in domain IV	Very membrane proximal	[33,46]
F265	scFv	EGFRvIII	n.d. (27.5 nM)[a]	Unknown	Domain I/III neoepitope, non-competitive with F269	Membrane distal	[29] and unpublished
F269	scFv	EGFRvIII	n.d. (31.5 nM)[a]	Unknown	Domain I/III neoepitope of EGFR, non-competitive with F265	Membrane distal	[29] and unpublished

[a]Binding of scFvs was not evaluated. Monovalent affinity of full-length IgG is shown in parentheses.
Cyno: cynomolgus monkey

bioRxiv preprint doi: https://doi.org/10.1101/2020.10.30.360925; this version posted October 30, 2020. The copyright holder for this preprint (which was not certified by peer review) is the author/funder, who has granted bioRxiv a license to display the preprint in perpetuity. It is made available under aCC-BY-NC-ND 4.0 International license.

Figure Legends

Figure 1: Identification of EGFR-specific sdAbs with CAR functionality. (A) The structural elements of human EGFR and sdAb based EGFR-targeting CAR tested here are shown. Various EGFR-specific sdAbs were cloned into a modular CAR backbone via golden gate cloning. Jurkat cells were then electroporated with the resulting constructs. Control cells with no plasmid or with a CD19-targeted scFv element were also tested here (FMC63-28z). Jurkat cells (30 000/well) transiently expressing various CAR plasmids as shown were co-cultured with varying doses of (B) EGFR-high SKOV3 cells, (C) EGFR-low MCF7 cells, or (D) EGFR-negative Raji cells and examined for activation via staining with APC-labelled anti-human CD69 antibody. Results show the mean +/- SEM from a single experiment performed in duplicate.

Figure 2: Hinge truncation decreases target response for EGFR-sdAb CAR constructs. (A) Single domain antibody based CARs targeting human EGFR were generated with hinge domains of varying length [full length human CD8-hinge (45CD8h), truncated CD8-hinge (34CD8h or 22CD8h), or no hinge element. (B-D) Jurkat cells were electroporated with varying CAR constructs before co-incubation with no target cells (1:0 E:T), EGFR-high SKOV3 cells, or EGFR-low MCF7 cells. After overnight incubation CAR/GFP+ cells were examined for activation via staining with APC-labelled anti-human CD69 antibody. Results show the mean +/- SEM from a single experiment performed in duplicate.

Figure 3: CAR hinge sensitivity is highly dependent on target antigen and epitope location. (A) A range of sdCAR constructs were produced containing the EGFR-specific sdAb021 and human CD8 hinge domains ranging between 1 and 45 residues in length. The full-length 45-residue CD8 hinge was extended with a Gly-Ser linker between 1 and 17 residues in length. Jurkat cells were electroporated with the resulting constructs and then co-incubated at an effector to target ratio of 1:1 with EGFR-high SKOV3 cells, EGFR-low MCF7 cells, or EGFR-negative NALM6 cells. After overnight incubation, CAR/GFP+ cells were examined for activation via staining with APC-labelled anti-human CD69 antibody. (B) Similarly, trastuzumab-scFv HER2-specific CAR constructs were generated with hinge domains of varying lengths. CAR-expressing Jurkat cells were co-incubated with HER2-high SKOV3 cells, HER2-low MCF7 cells, or HER2-negative NALM6 cells and then CAR-T activation was assessed. (C) Similarly, EGFRvIII-specific CAR constructs were generated with hinge domains of varying lengths. CAR-expressing Jurkat cells were co-incubated with EGFRvIII-overexpressing U87vIII cells or EGFRvIII-negative U87wt cells and then CAR-T activation was assessed. Results show means +/- SEMs of three separate experiments.

Figure 4: Hinge truncation progressively diminishes tumor cell killing and expansion of primary sdCAR-T cells in response to EGFR expressing cells. Concentrated lentiviral particles encoding hinge-modified EGFR-specific sdAb021 CARs as well as a GFP marker were generated. Peripheral blood T cells were isolated from two donors before polyclonal expansion and lentiviral transduction. Varying doses of sdCAR-T cells or mock transduced cells (empty CAR backbone lentivirus) were added to a 96-well plate containing 2000 EGFR-high SKOV3, EGFR-medium U87vIII, or EGFR-low MCF7 target cells stably expressing nuclear localized mKate2 (red). Co-cultures were examined over 7 days via live fluorescence microscopy (Incucyte) to differentiate (A-B) red-fluorescent target cell counts or (C-D) total area of green-fluorescent CAR-T cells. (E) Fold changes in target cell expansion and (F) CAR-T cell expansion at day 5 for are summarized at varying effector:target ratios. Each graph depicts automated cell counts or fluorescent areas from a single well from a single experiment.

Figure 5: Hinge-truncated sdCAR-T cells maintain selectivity for EGFR overexpressing cells following re-challenge. Donor blood derived T cells were transduced with lentiviral particles encoding the EGFR-

bioRxiv preprint doi: https://doi.org/10.1101/2020.10.30.360925; this version posted October 30, 2020. The copyright holder for this preprint (which was not certified by peer review) is the author/funder, who has granted bioRxiv a license to display the preprint in perpetuity. It is made available under aCC-BY-NC-ND 4.0 International license.

specific sdAb021 sdCAR with varying hinge domains. The resulting sdCAR-T cells were challenged via co-culture with EGFR-high SKOV3 cells and examined for (A) target cell expansion or (B) sdCAR-T cell expansion as described above. Challenged cells were then diluted 1/10 with fresh media and challenged with (B,E) EGFR-high SKOV3 cells, (G,I) EGFR-medium U87vIII cells, or (K, M) EGFR-low MCF7 cells. Similarly, cells challenged twice with SKOV3 cells were re-challenged with various target cells and examined for (C,H,L) target cell expansion and (F,J,N) CAR-T cell expansion. Each graph depicts automated cell counts or fluorescent areas from a single well from a single experiment.

Figure 6: Hinge truncated EGFR sdCAR-T cells show progressively diminished response to target cells in vivo. NOD/SCID/IL2γ-chain-null (NSG) mice were injected subcutaneously with 2×10^6 SKOV3 cells stably expressing mKate2. Mice were injected with 5×10^6 total T cells (~$1x10^6$ CAR-T cells) intravenously. (A) Tumor volume was estimated using caliper measurements and (B) time to defined humane endpoint (tumor volume 2000 mm^3) was assessed. Δ, The experiment was ended early due to COVID-19 related animal facility shutdown, and thus the final tumor measurement of day 112 is shown in (C). (D) Fluorescence imaging was performed at varying timepoints after tumor cell injection. (E) Blood was also collected at selected timepoints after tumor challenge to quantify the proportion of human CD45+ cells that were GFP/CAR+. (F) Staining for human CCR7 and CD45RA was used to assess the differentiation status of CAR/GFP+ cells or total T cells for mice treated with mock-transduced CAR-T cells. See inset for gating strategy used to delineate effector, naïve, central memory, or effector memory-RA+ (EMRA) cells.

bioRxiv preprint doi: https://doi.org/10.1101/2020.10.30.360925; this version posted October 30, 2020. The copyright holder for this preprint (which was not certified by peer review) is the author/funder, who has granted bioRxiv a license to display the preprint in perpetuity. It is made available under aCC-BY-NC-ND 4.0 International license.

Supplementary Figure Legends

Supplementary Figure 1: Measurement of surface EGFR expression on MCF7, U87vIII, and SKOV3 cells via flow cytometry. Jurkat, MCF7, U87vIII, and SKOV3 cells were stained with varying amounts of commercial PE-CF594 anti-human EGFR antibody (0.4mg/mL) and examined by flow cytometry as indicated. Results demonstrated very high expression for SKOV3, slightly lower expression in U87vIII, low expression in MCF7 cells, and no expression in Jurkat cells. Histograms depict the fluorescence signal from a single experiment.

Supplementary Figure 2: Relationship between hinge length and EGFR sdCAR response against EGFR-high and EGFR-low target cells. (A) Data presented for CAR-J assay against EGFR-high SKOV3 cells as described in figure 2 were reorganized here to show the activation of EGFR sdCARs over a range of hinge lengths at an effector to target ratio of 1:10, varying from a full 45 amino acid human CD8 hinge to no hinge. (B) Data from CAR-J data against EGFR-low MCF7 cells organized via hinge length are shown. (C) The relative selectivity of hinge-modified EGFR sdCARs for SKOV3 over MCF7 is shown. Results depict the mean +/- SEM of a single experiment performed in duplicate.

Supplementary Figure 3: sdCAR auto-activation shows no consistent association with hinge length. CAR-J activation data for the EGFR sdAb021 hinge-modified sdCARs with no target cells or with EGFR-negative NALM6 cells is shown. Results show the means +/- SEMs of three independent experiments.

Supplementary Figure 4: Hinge truncation results in reduced response to antigen-low target cells with no consistent change in sdCAR tonic signaling. (A and B) Primary sdCAR-T cells were generated from two independent blood donors as described in the text and placed at low density in a 96-well plate. Cells were then monitored for growth via live fluorescence microscopy over 7 days. Graphs display the total areas of GFP+ cells as enumerated through automated cell counting. (C) Representative images are provided for various sdCAR-T (GFP/green) or control mock T cells with target cell (mKate2/red) co-cultures 4 days after plating at an effector:target ratio of 5:1.

Supplementary Figure 5: Hinge truncation results in similar progressively diminished EGFR-specific sdCAR activity in the more aggressive U87vIII xenograft tumor model. (A) NSG mice were injected subcutaneously with 1×10^6 U87vIII cells stably expressing mKate2. At 7 and 14 days post-tumor challenge mice were injected intratumorally with 1×10^7 total T cells (approx. 2.5×10^6 hinge-modified sdCAR-T cells) or with untransduced control T cells (mock). Tumor growth was monitored via caliper measurements. N=5 mice per group. (B) Mice were sacrificed at pre-determined endpoints based on animal condition or tumor volume >2000 mm^3. (C) In vivo imaging was performed to examine the mKate2 fluorescent signal associated with tumor cells. (D) Blood was drawn from challenged mice and examined for the proportion of sdCAR-transduced cells (GFP+) within the hCD45+ lymphocyte fraction at the final timepoint where all experimental mice were alive (day 21). (E) sdCAR-T cells, or total hCD45+ cells for mock T cell treated mice, were examined for differentiation status using antibody staining for human CCCR7 and CD45RA. See inset for gating strategy used to delineate effector, naïve, central memory, or effector memory-RA+ (EMRA) cells.

Supplementary Figure 6: Workflow for discovery and optimization of novel tumor selective sdCAR constructs: Antigen preparation, llama immunization, phage library preparation and panning, cell binding, CAR cloning, high-throughput CAR screening, and fine-tuning of CAR signaling in Jurkat cells through hinge length modulation was performed for several novel EGFR sdCAR constructs.

bioRxiv preprint doi: https://doi.org/10.1101/2020.10.30.360925; this version posted October 30, 2020. The copyright holder for this preprint (which was not certified by peer review) is the author/funder, who has granted bioRxiv a license to display the preprint in perpetuity. It is made available under aCC-BY-NC-ND 4.0 International license.

Subsequently, confirmatory experiments were performed to test lead sdCARs in vitro and in vivo using primary human CAR-T cells.

bioRxiv preprint doi: https://doi.org/10.1101/2020.10.30.360925; this version posted October 30, 2020. The copyright holder for this preprint (which was not certified by peer review) is the author/funder, who has granted bioRxiv a license to display the preprint in perpetuity. It is made available under aCC-BY-NC-ND 4.0 International license.

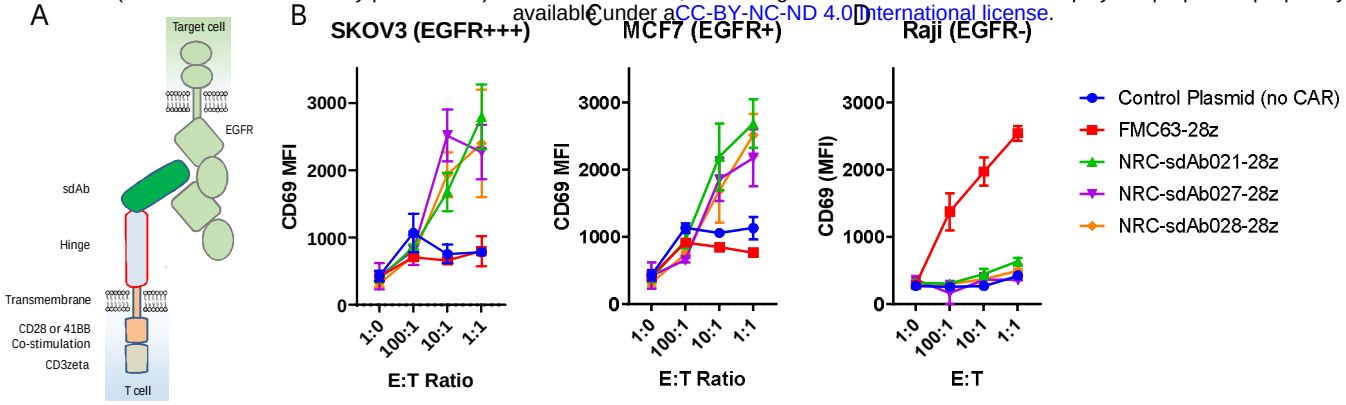

Figure 1: Identification of EGFR-specific sdAbs with CAR functionality

bioRxiv preprint doi: https://doi.org/10.1101/2020.10.30.360925; this version posted October 30, 2020. The copyright holder for this preprint (which was not certified by peer review) is the author/funder, who has granted bioRxiv a license to display the preprint in perpetuity. It is made available under aCC-BY-NC-ND 4.0 International license.

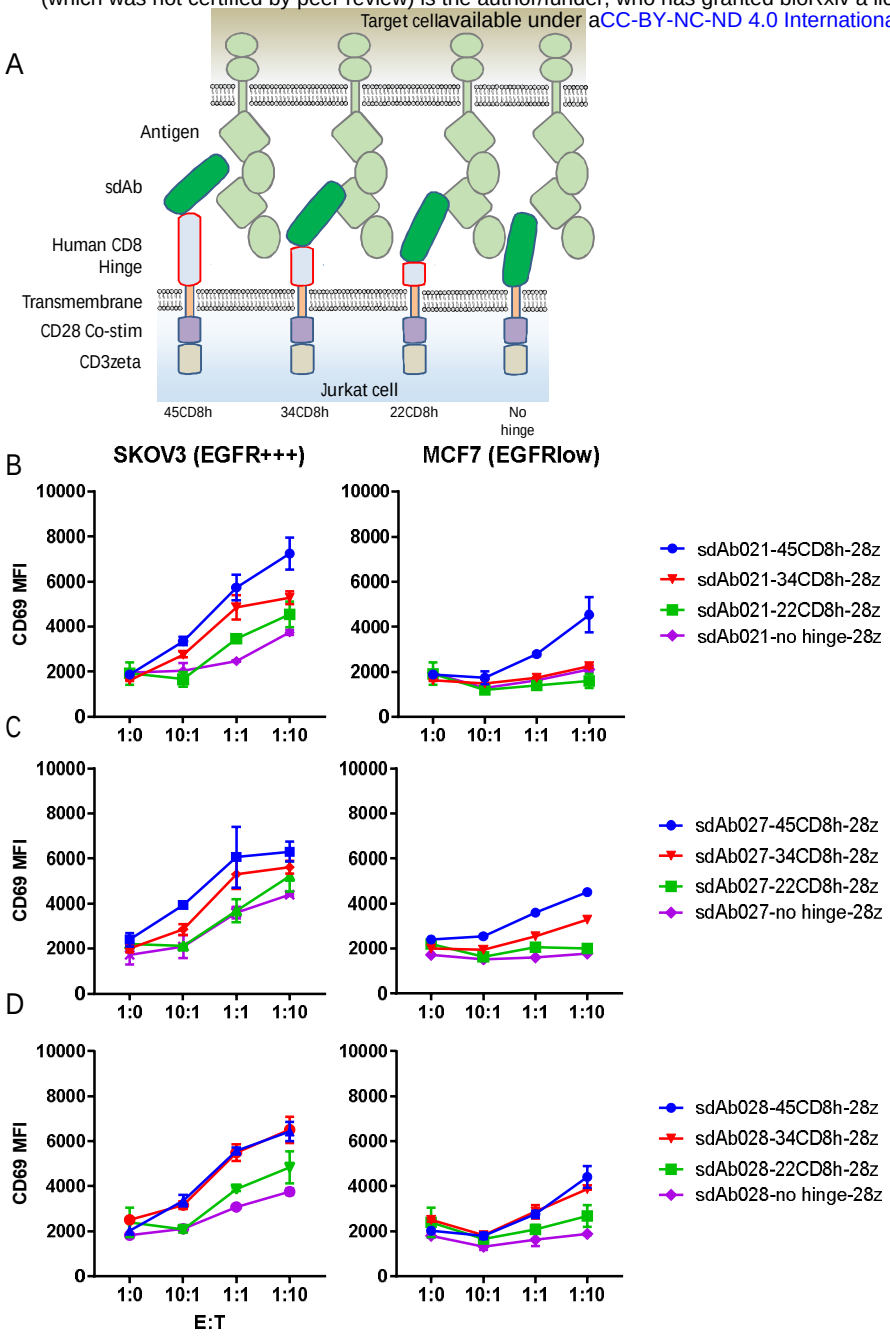

Figure 2: Hinge truncation decreases target response for EGFR-sdAb CAR constructs

bioRxiv preprint doi: https://doi.org/10.1101/2020.10.30.360925; this version posted October 30, 2020. The copyright holder for this preprint (which was not certified by peer review) is the author/funder, who has granted bioRxiv a license to display the preprint in perpetuity. It is made available under aCC-BY-NC-ND 4.0 International license.

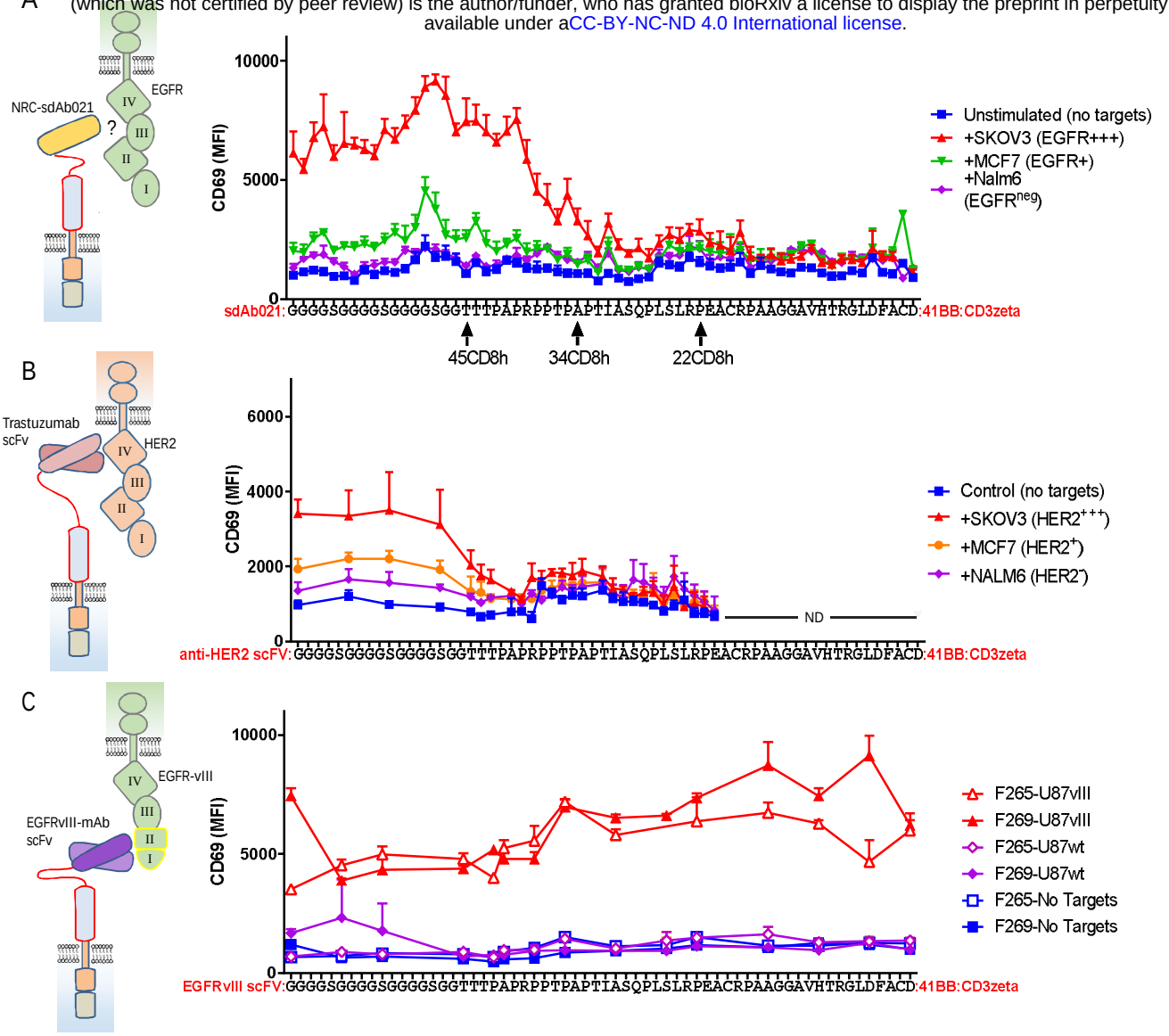

Figure 3: CAR Hinge Sensitivity is Highly Dependent on Epitope Location

bioRxiv preprint doi: https://doi.org/10.1101/2020.10.30.360925; this version posted October 30, 2020. The copyright holder for this preprint (which was not certified by peer review) is the author/funder, who has granted bioRxiv a license to display the preprint in perpetuity. It is made available under aCC-BY-NC-ND 4.0 International license.

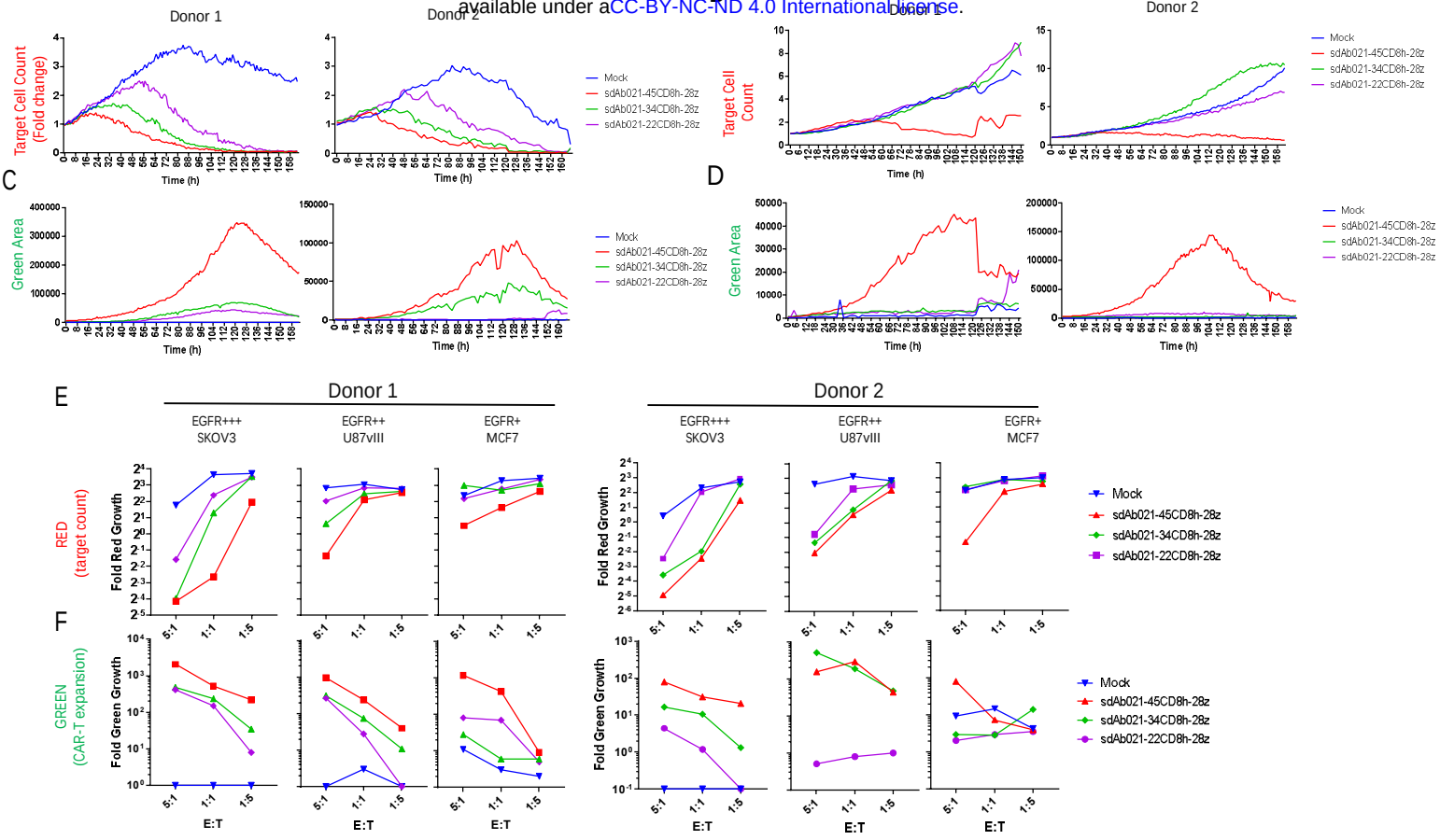

Figure 4: Hinge truncation progressively diminishes tumour cell killing and expansion of primary CAR-T cells in response to target expressing cells

bioRxiv preprint doi: https://doi.org/10.1101/2020.10.30.360925; this version posted October 30, 2020. The copyright holder for this preprint (which was not certified by peer review) is the author/funder, who has granted bioRxiv a license to display the preprint in perpetuity. It is made available under aCC-BY-NC-ND 4.0 International license.

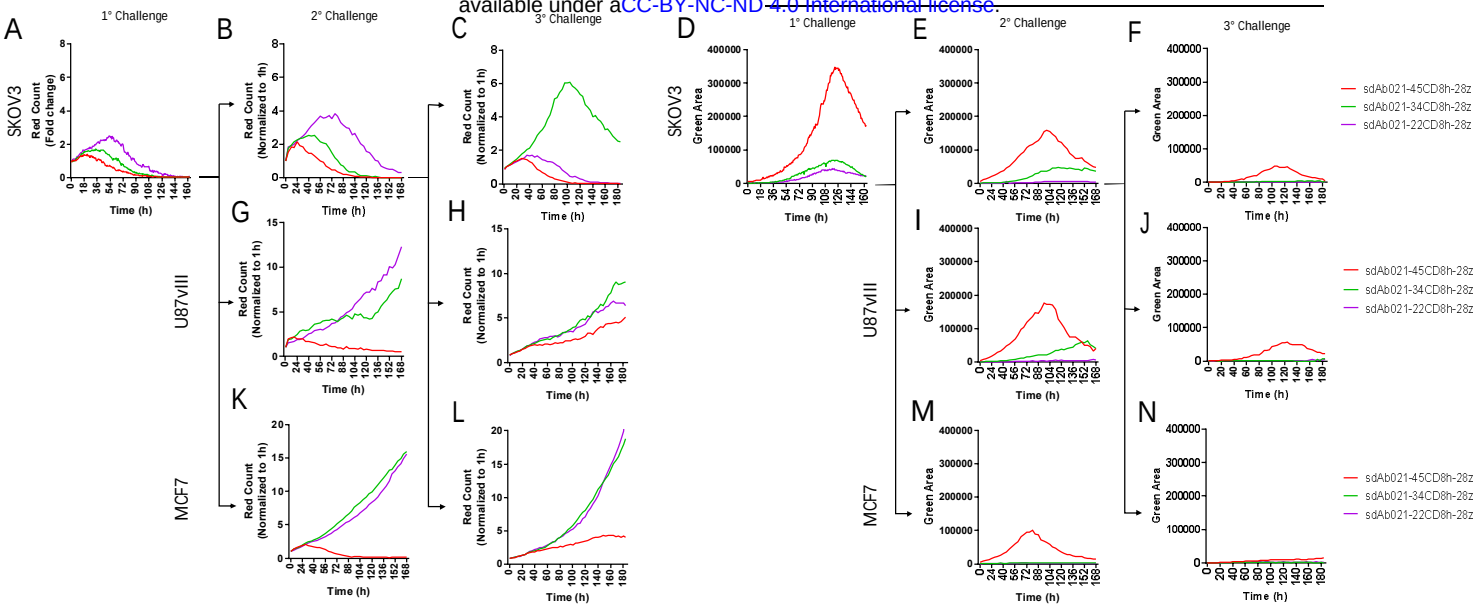

Figure 5: Hinge truncated CAR-T cells maintain selectivity for target overexpressing cells following re-challenge

bioRxiv preprint doi: https://doi.org/10.1101/2020.10.30.360925; this version posted October 30, 2020. The copyright holder for this preprint (which was not certified by peer review) is the author/funder, who has granted bioRxiv a license to display the preprint in perpetuity. It is made available under aCC-BY-NC-ND 4.0 International license.

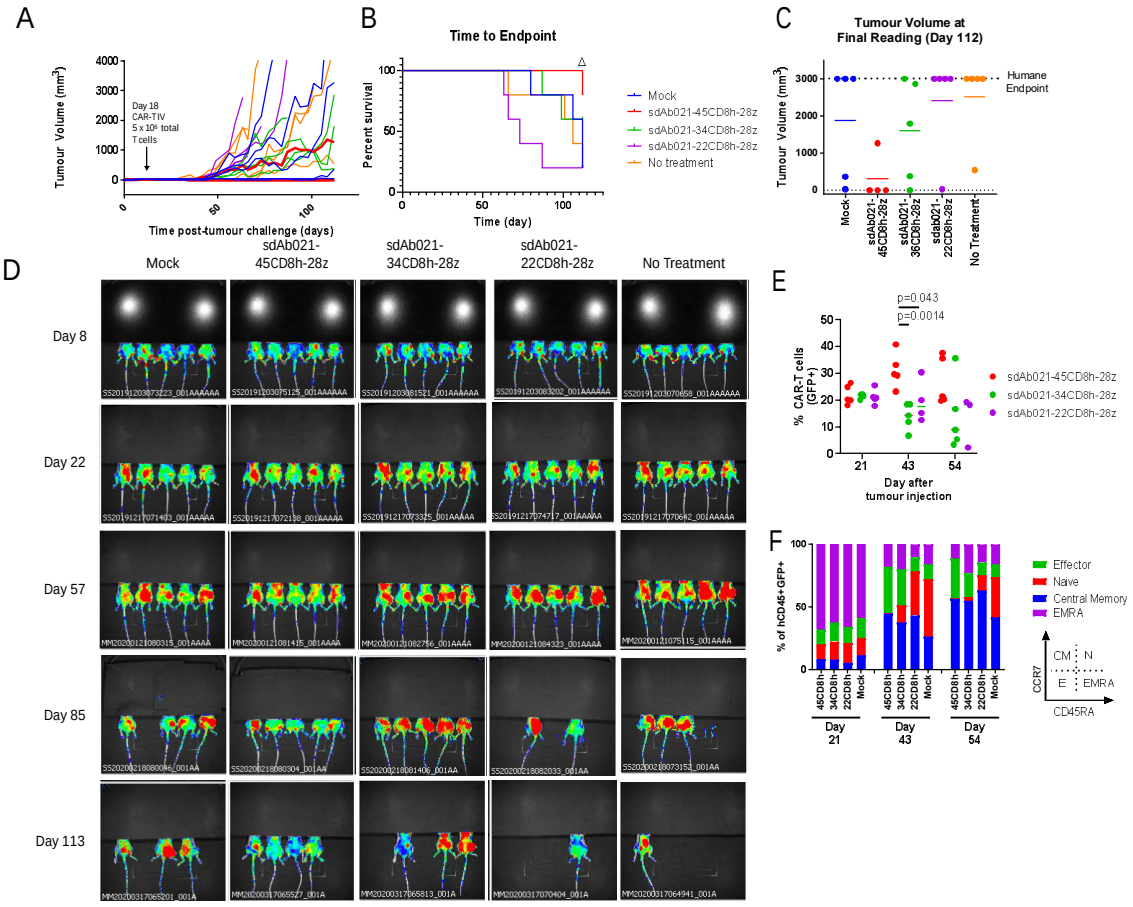

Figure 6: Hinge truncated CAR-T cells show progressively diminished response to target overexpressing cells in vivo

bioRxiv preprint doi: https://doi.org/10.1101/2020.10.30.360925; this version posted October 30, 2020. The copyright holder for this preprint (which was not certified by peer review) is the author/funder, who has granted bioRxiv a license to display the preprint in perpetuity. It is made available under aCC-BY-NC-ND 4.0 International license.

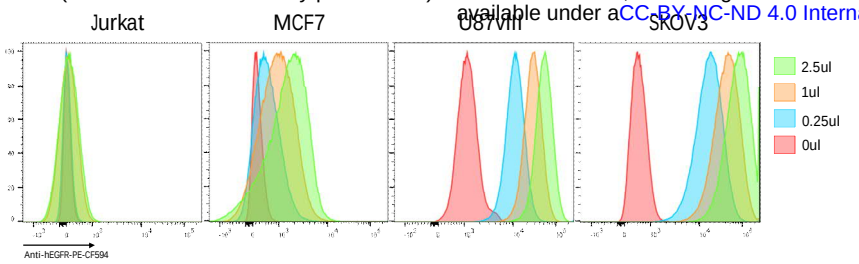

Supplemental Figure 1: Measurement of surface EGFR expression on MCF7, U87vIII, and SKOV3 cells via flow cytometry

bioRxiv preprint doi: https://doi.org/10.1101/2020.10.30.360925; this version posted October 30, 2020. The copyright holder for this preprint (which was not certified by peer review) is the author/funder, who has granted bioRxiv a license to display the preprint in perpetuity. It is made available under a CC-BY-NC-ND 4.0 International license.

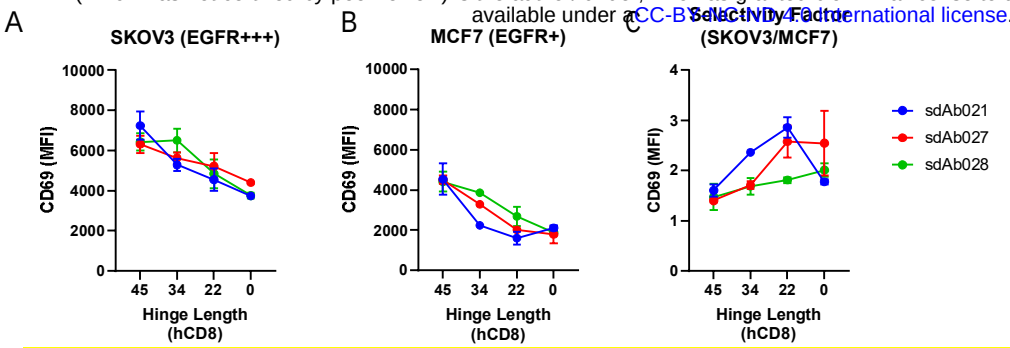

Supplemental Figure 2: Relationship between hinge length and CAR response in EGFR-high and EGFR-low target cells

bioRxiv preprint doi: https://doi.org/10.1101/2020.10.30.360925; this version posted October 30, 2020. The copyright holder for this preprint (which was not certified by peer review) is the author/funder, who has granted bioRxiv a license to display the preprint in perpetuity. It is made available under aCC-BY-NC-ND 4.0 International license.

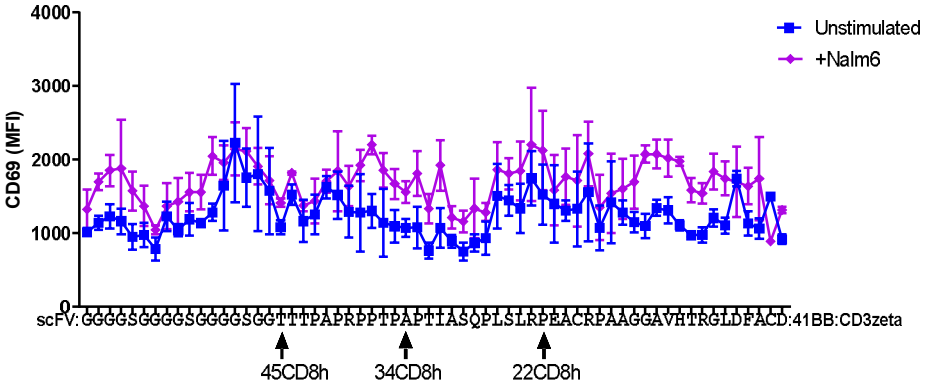

Supplemental Figure 3: CAR auto-activation shows no consistent pattern with hinge length

bioRxiv preprint doi: https://doi.org/10.1101/2020.10.30.360925; this version posted October 30, 2020. The copyright holder for this preprint (which was not certified by peer review) is the author/funder, who has granted bioRxiv a license to display the preprint in perpetuity. It is made available under aCC-BY-NC-ND 4.0 International license.

A

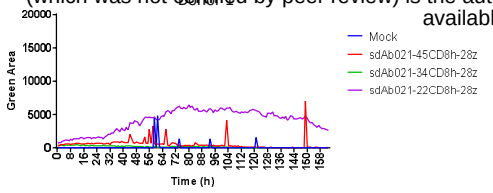

B

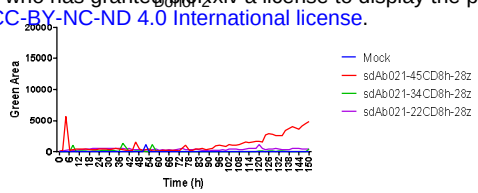

C

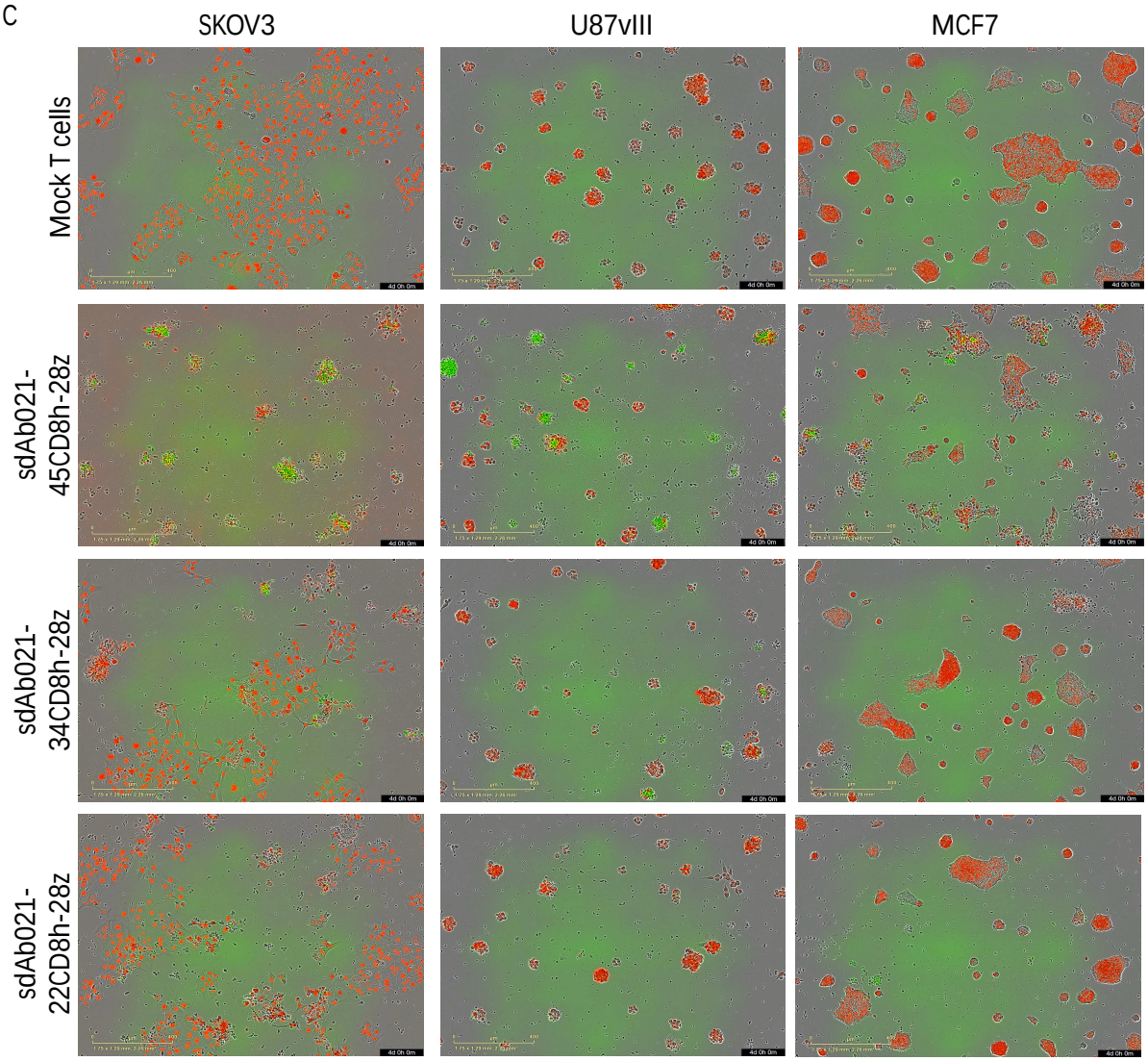

Supplemental Figure 4: Hinge truncation results in reduced response to antigen-low target cells with no consistent change CAR tonic signaling

bioRxiv preprint doi: https://doi.org/10.1101/2020.10.30.360925; this version posted October 30, 2020. The copyright holder for this preprint (which was not certified by peer review) is the author/funder, who has granted bioRxiv a license to display the preprint in perpetuity. It is made available under aCC-BY-NC-ND 4.0 International license.

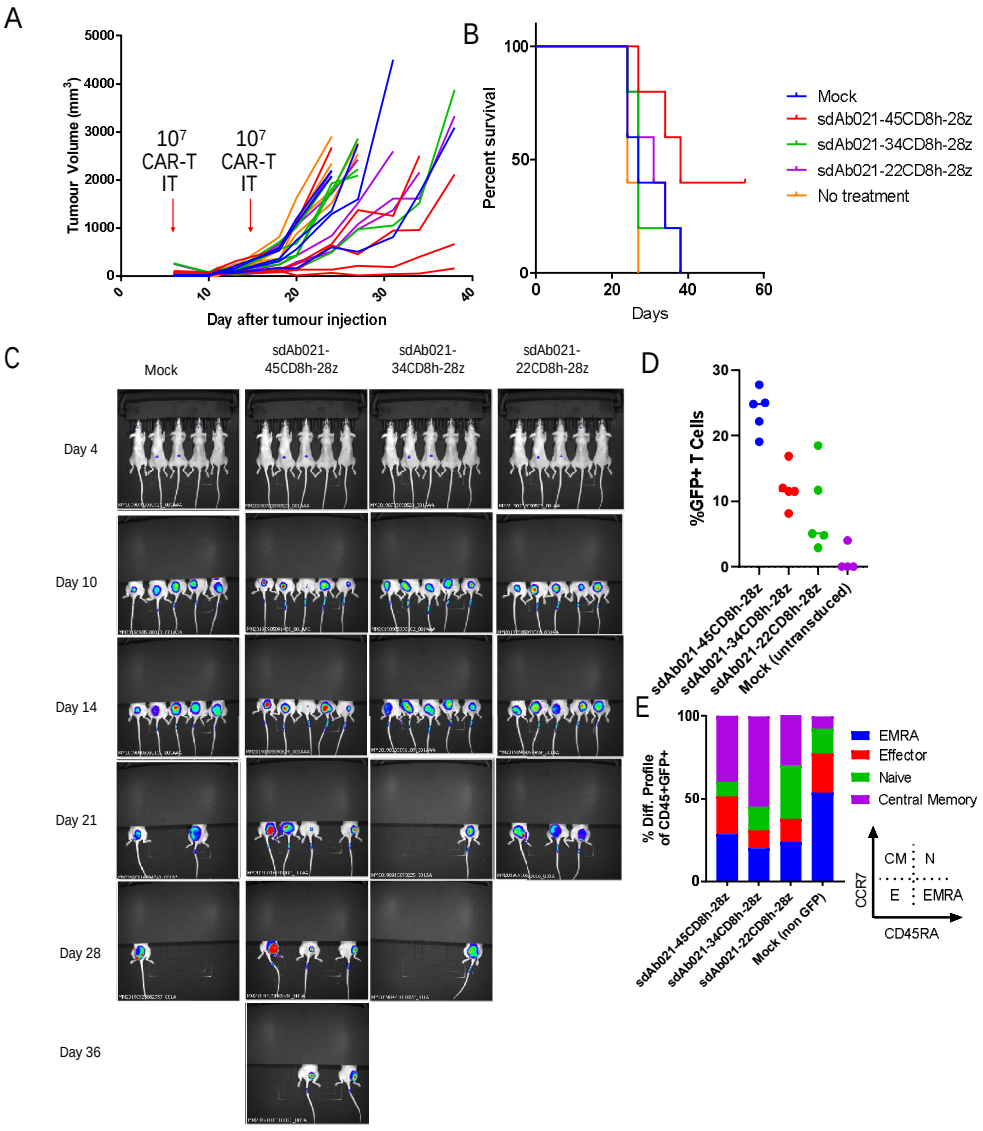

Supplementary figure 5: Hinge truncation produces similar progressively diminished activity in the more aggressive U87vIII xenograft tumour model

bioRxiv preprint doi: https://doi.org/10.1101/2020.10.30.360925; this version posted October 30, 2020. The copyright holder for this preprint (which was not certified by peer review) is the author/funder, who has granted bioRxiv a license to display the preprint in perpetuity. It is made available under aCC-BY-NC-ND 4.0 International license.

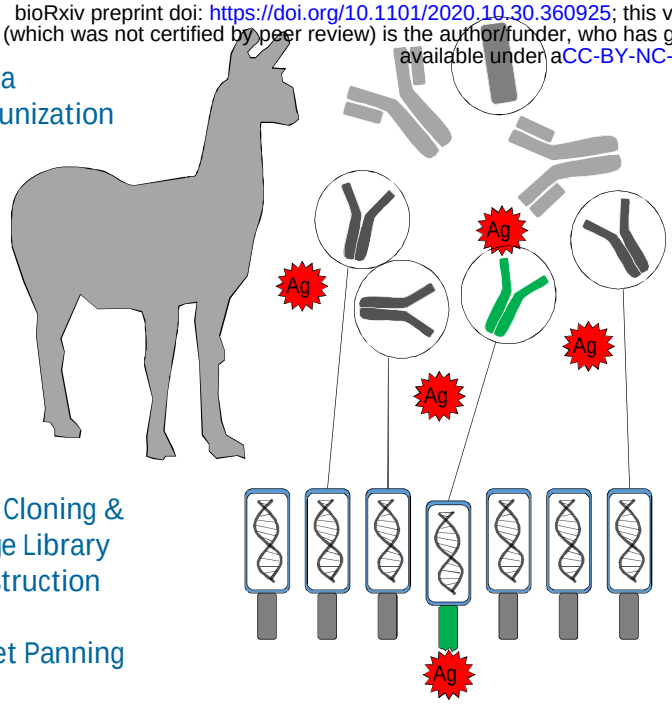

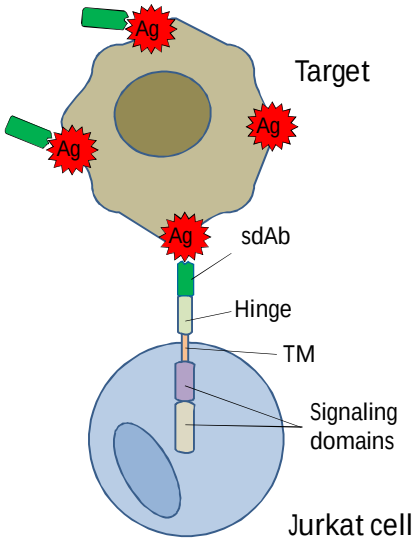

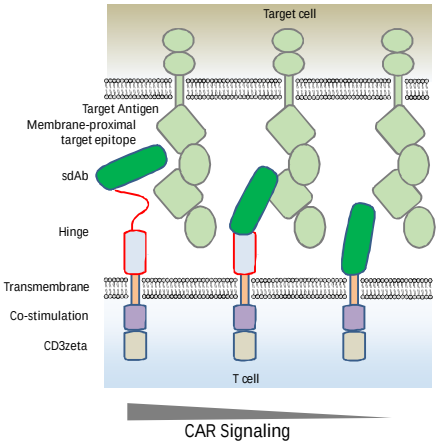

In vitro and in vivo confirmatory testing using primary human CAR-T cells

Supplementary figure 6: Workflow diagram for discovery and optimization for novel tumour selective CAR constructs

bioRxiv preprint doi: https://doi.org/10.1101/2020.10.30.360925; this version posted October 30, 2020. The copyright holder for this preprint (which was not certified by peer review) is the author/funder, who has granted bioRxiv a license to display the preprint in perpetuity. It is made available under aCC-BY-NC-ND 4.0 International license.

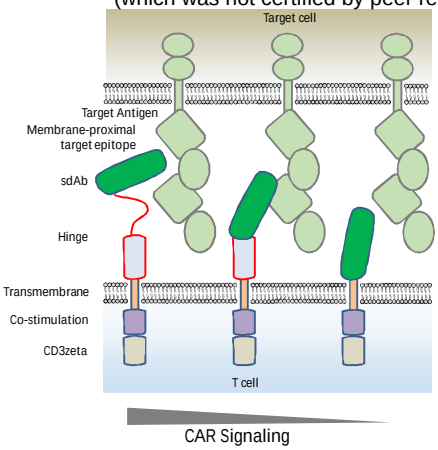

Graphical Abstract